Physicochem. Probl. Miner. Process., 60(3), 2024, 189958

http://www.journalssystem.com/ppmp

Physicochemical Problems of Mineral Processing

ISSN 1643-1049

Effect of two-stage energy input on enhancing the flotation process of high-ash coal slime

Xing Wang [1,2], Youli Han [1,2], Jinbo Zhu [1,2], Lingyun Liu [1,2], Hongyang Wang [1,3], Zhiyong Lin[1], Shuwei Xia [1], Po Wang [4]

[1] School of Material Science and Engineering, Anhui University of Science and Technology, Huainan 232001, China

[2] Anhui Engineering Research Center for Coal Clean Processing and Carbon Emission Reduction, Huainan 232001, China

[3] State Key Laboratory of Mineral Processing, Beijing 100260, China

[4] Linhuan Coal Preparation Plant, Huaibei Mining Group, Huaibei, Anhui 235000, China

Corresponding authors: yolhan@163.com (Youli Han), jinbzhu@163.com (Jinbo Zhu)

Abstract: To solve the mismatch problems of nonlinear changes of coal slurry properties and energy input during the continuous flotation process, a two-stage energy input method was used to promote the efficient recovery of clean coal and achieve maximized benefits. Results showed that the flotation rate constant increased with the increase in stirring speed and reached its maximum value of 0.0271 s^{-1} when the stirring speed increased to 1200 r/min under a single energy input, with a maximum combustible recovery of 74.35%. However, the short-term flotation results within 40 s showed that the combustible recovery increased with stirring speed and reached its maximum value of 50.19% at 1500 r/min. The stirring speed was set at 1800 r/min for a fast flotation period and 2400 r/min for an enhanced separation period, which could achieve a maximum combustible recovery of 89.21%. Furthermore, the adsorption density of the collector was optimized, exceeding that achieved under single-stage energy input. The flotation process could be optimized by two-stage energy input. Coarse coal particles were preferentially floated by low-speed stirring in the initial fast selection period. Fine coal particles were further separated during the enhanced separation period under the action of high-speed shear. Two-stage energy input could significantly improve the combustible recovery of the overall flotation of coal slime.

Keywords: flotation, high-ash coal slime, single stage energy input, two-stage energy input, combustible recovery

1. Introduction

Flotation technology plays a crucial role in treating coal slurry and is the focus of the industry's ongoing efforts to achieve high-efficiency recovery and high-value utilization of fine slime (Wan et al., 2023; Yue and Ren, 2022; Zhuo et al., 2023). A combined production process of "heavy media separation + flotation" is usually used in coking coal preparation plants. Raw coal particles with size larger than 0.5 mm are treated by dense medium process, whereas coal slurry particles smaller than 0.5 mm are recovered by flotation technology. In some central coal preparation plants, raw coal comes from more than 10 surrounding mines. The washed raw coal includes coking coal, fat coal, lean coal, and 1/3 coking coal. The quality of the selected raw coal varies considerably, posing a significant challenge to quality control (Guo et al., 2022). The raw coal contains numerous associated gangue minerals, such as kaolinite, montmorillonite, and illite (Abbaker and Aslan, 2023). These minerals are prone to argillization in the separation process, resulting in the deterioration of fine slime separation environment(Jung et al., 2023).

The increase in the fine mud content aggravates the difficulty of flotation production, resulting in a high-ash flotation concentrate and the serious "back ash" phenomenon in heavy medium cleaned coal, which affects the final quality of cleaned coal(Sun et al., 2021). In recent years, scholars have paid attention to the problem of fine slime pollution in clean coal flotation and carried out extensive experimental and theoretical research (Xia et al., 2020a), They demonstrated that the problem of fine

DOI: 10.37190/ppmp/189958

coal slime pollution in high-ash coal slime can be effectively removed by refined flotation to improve the flotation quality (Barraza et al., 2013). The contamination of fine gangue in flotation concentrate typically occurs through water entrainment, fine mud cover, and mechanical entrainment (Yu et al., 2017). Bubble–particle attachment tests with coal particles also indicated that fine clay particles increase the attachment time between an air bubble and the coal particles and significantly reduce the efficiency of bubble–coal attachment and the coal flotation recovery (Oats et al., 2010). Increasing turbulence is beneficial to particle–bubble collision but detrimental to stabilizing particle–bubble aggregates (Yao et al., 2021), where turbulence with intensive energy dissipation rate is favored for the flotation of coal slime particle, improved desorption of fine slime on the coal surface, and enhanced separation kinetics and separation efficiency of the slime (Hassanzadeh et al., 2022; Zhao et al., 2022). The strong stirring flow mode is beneficial in enhancing three-phase mixing, inter-particle and particle-reagent interactions, and hydrophobicity of the required particles (Kadagala et al., 2021). High fluid shear rate further disperses particles and agents, and promotes their ability to be adsorbed quickly and selectively onto the coal surfaces (Zhou et al., 2023), The increased opportunity for reagent adsorption is mainly due to the reduced interfacial tension between oil and water, particularly in oxidized or low-rank coals (Kadagala et al., 2021). The strong shear force generated in the slurry mixing process can effectively remove the cover of gangue minerals such as kaolinite on the surface of coal particles(Li et al., 2021; Li et al., 2019), and increase the direct adsorption area of the collector on the surface of coal slime particles. In coal slime flotation, kerosene, diesel, and other non-polar hydrocarbon oils are typically used as collectors in the form of oily collector pre-dispersions to improve the adsorption of oil molecules. This step can enhances the flotation recovery by 5%–10% compared with the traditional flowsheet (Xia et al., 2020b). The adsorption of non-polar hydrocarbon oils on the surface of coal slime particles is mainly physical adsorption, which is characterized by its weak nature and susceptibility to desorption (Han et al., 2022; Laskowski et al., 2007). Therefore, some scholars have studied the effective adsorption probability of collectors on the surface of coal slime and found that it is affected by the theoretical collision probability of particles, probability of particles flowing around, and probability of desorption after adsorption (Pan et al., 2023; Wang et al., 2022). The energy input in the pulp mixing process influences the effective adsorption probability of the reagent, which implied that the surface hydrophobicity of coal particles can be strengthened by the flotation intensification with preconditioning (Hazare et al., 2023). In addition, an optimal droplet size (7.68 μm) was found, at which the coal flotation performance was maximized; beyond this size, the flotation performance deteriorated (Liu et al., 2023; Yang et al., 2018). An optimal equilibrium state between the adsorption rate and separation rate of the particles and reagents needs to be achieved by adjusting energy input; low stirring speeds are beneficial for particles with low hydrophobicity as they increase the contact time between the agent and the particles (Koh and Smith, 2011). The flotation process is a continuous evolving separation environment where minerals that are inherently easier to float tend to separate promptly while those that are inherently more challenging to float remain suspended within the pulp environment. Consequently, variable energy inputs must be introduced during the flotation process to cater to the nonlinear fluctuations in pulp properties and optimize the overall recovery efficiency(Gui et al., 2017; Hassanzadeh et al., 2022; Yang et al., 2020b).

This study realizes the dynamic adjustment of the flotation flow field by changing the speed of the flotation machine. By transforming the laboratory XFD-1.5 flotation, the influence of single-stage energy input and two-stage energy input on the flotation test results of high-ash coal slime was studied. The characteristics of mineral composition in the rapid flotation period and the enhanced separation period were analyzed to provide theoretical and technical guidance for the efficient separation of high-ash coal slime.

2. Experimental

2.1. Experimental device

Flotation experiments were conducted in a mechanical flotation machine with 1.5 L cell volume. The diagram of the flotation test system is shown in Fig. 1, which comprised three parts: (1) a three-phase motor used to output different stirring speeds; (2) a frequency converter used to control the working frequency of the three-phase motor; and (3) flotation tests performed in an XFD flotation machine.

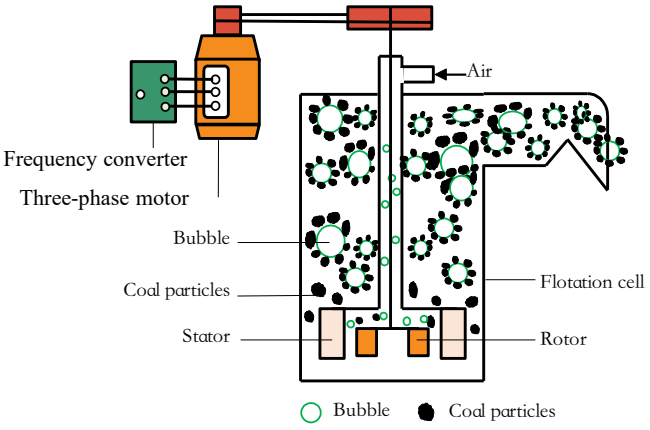

Fig. 1. Diagram of the flotation test system

2.2. Test samples

2.2.1. Screen test

This study employed high-ash flotation tailing coal samples from the Linhuan coal preparation plant in Anhui Province, China. The ash content of the samples was 49.32%. The particle size composition of the samples was analyzed using the "coal screening test method." Table 1 shows its size composition. The yield of coarse particles of >0.125 mm was 11.93%, with ash of 15.17%. These values suggested that the low-ash coarse particles of >0.125 mm were not entirely recovered by the coarse slime system, resulting in a small amount of coarse particles lost in the coal slime. Moreover, the yield of <0.075 mm coal sample was 79.54% with an ash content of 57.37%, indicating that <0.075 mm was the dominant grain size. However, the yield of the >0.075 mm particle size fraction was 20.46%, and its comprehensive ash content was 18.01%, which was relatively low and could be further recovered.

Table 1. Particle size composition of flotation coal samples

Size fraction/mm	Weight/%	Ash/%	Cumulative retained/%		Cumulative passing/%	
			Weight	Ash	Weight	Ash
0.500~0.250	0.85	15.05	0.85	15.05	100.00	49.32
0.250~0.125	11.08	15.18	11.93	15.17	99.15	49.62
0.125~0.075	8.52	21.98	20.46	18.01	88.07	53.95
0.075~0.045	7.57	35.73	28.02	22.79	79.54	57.37
0.045~0	71.98	59.65	100.00	49.32	71.98	59.65
Total	100.00	49.32				

2.3. Float-and-sink analysis

The particle density composition of flotation tailings was analyzed using the float-and-sink test. Table 2 shows that 24.97% by weight of the coal slime particles had a density greater than 1.8 g.cm^{-3}, with an ash content of 88.07%. These particles were categorized as high-ash gangue products and useless minerals. Conversely, the coal slime yielded 24.33% for particles with a density of <1.4 g.cm^{-3}, and a comprehensive ash content of 11.10%, allowing for recycling as clean coal products. The proportion of 1.4-1.8 g.cm^{-3} density material in coal slime was 50.70% with ash content of 48.58%. If the low ash coal with a density of less than 1.4 g.cm-^{3} was further recovered, the tailings increased from 49.32% to 61.61%, thereby increasing the yield of clean coal and the ash of tailings.

2.4. XRD analysis

The XRD pattern of the coal sample is shown in Fig. 2. The main clay minerals in coal slime were kaolinite, montmorillonite, and quartz. The particle size of gangue minerals was easily reduced, and

mud formed in the presence of water, which deteriorated the separation environment of slime water. In the coal slime slurry, the clay mineral particles adhered to the surface of the coal particles, inhibiting the hydrophobic modification of the surface of the fine coal particles.

Table 2. Float-and-sink test results of coal samples

Density level/(g.cm^{-3})	Weight/%	Ash/%	Cumulative float/%		Cumulative sink/%	
			Weight	Ash	Weight	Ash
<1.3	11.42	9.24	11.42	9.24	100.00	49.32
1.3-1.4	12.91	12.75	24.33	11.10	88.58	54.49
1.4-1.5	9.15	20.34	33.48	13.63	75.67	61.61
1.5-1.6	14.93	37.48	48.41	20.98	66.52	67.29
1.6-1.8	26.62	64.52	75.03	36.43	51.59	75.92
>1.8	24.97	88.07	100.00	49.32	24.97	88.07
Total	100.00	49.32				

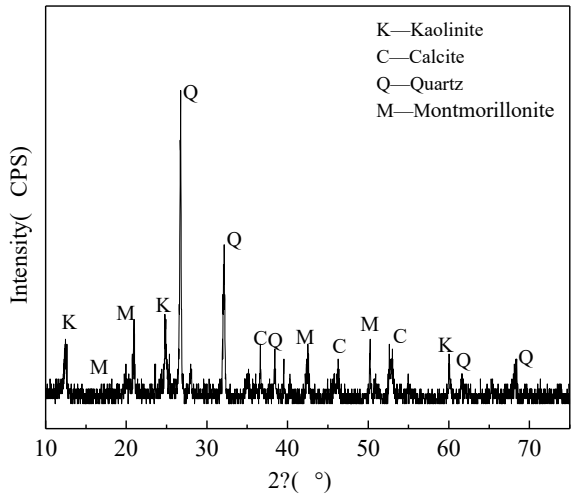

Fig. 2. XRD pattern of coal slurry

2.5. Methodology

2.5.1. Flotation test

The flotation test was carried out according to "The Method of Coal Slime Laboratory Unit Flotation Test" (GB/T 4757-2001). The flotation collector of diesel oil was 1000 g/t, and the 4-Methyl-2-pentanol was used as frother with the concentration of 100 g/t. The effect of agitation intensity on the flotation response of the coal slime was investigated at the stirring speeds of 600, 800, 1000, 1200, and 1500 r/min. The air rate was stably controlled to 0.2 m^3/(m^2.min) by using an external air pump with a pulp concentration of 80 g/L. After the coal samples were pre-wetted for 120 s, the collector was added for hydrophobic modification of the surface of the coal slime particles. The frother was added to the coal slurry after contact collision and adsorption of collector droplets with coal particles for 60 s. The froth removal time was 20, 20, 40, 40, 60, and 60 s. Six products (J_1, J_2, J_3, J_4, J_5, and J_6) were collected as clean coal, and one product (W) was tailings coal. The flowchart of the flotation rate test is shown in Fig. 3. Flotation concentrate yield (Y) and combustible recovery (R) were calculated by Formulas (1) and (2).

$$Y = \frac{m_c}{m_f} \times 100\% \quad (1)$$

$$R = \frac{Y(100-A_c)}{100-A_f} \quad (2)$$

where m_c is the mass of flotation concentrate, g; and m_f is the mass of flotation feed, g; A_c is the ash of flotation concentrate, %; and A_f is the ash of feed coal, %.

The first-order kinetic model was used to analyze the influence of the flotation machine shaft speed on the enhanced upgrading of high-ash flotation tailings, as shown in Formula(3) (Gui et al., 2017).

$$R = R_\infty(1 - e^{-kt}) \tag{3}$$

where R is the combustible recovery, %; R_∞ is the maximum value of R, %; k is the flotation rate constant, s^{-1}; and t is the flotation time, s.

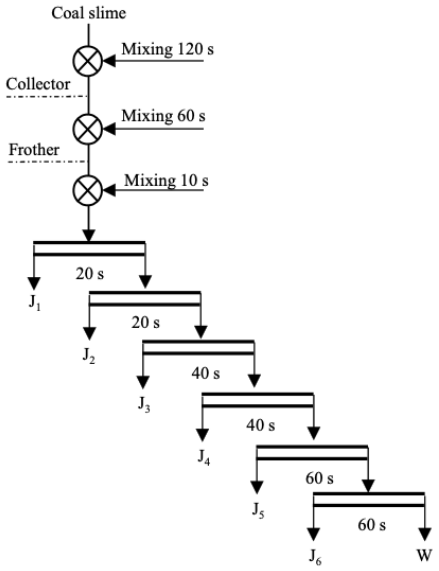

Fig. 3 Flowchart of flotation rate test

2.5.2. Adsorption measurements

The residual concentration method was used to measure the adsorption density of the collector diesel oil on coal particle surfaces. A dye treatment of 3 g of diesel oil and 0.1 g of Sudan red III was added to 50 mL of anhydrous ethanol for the preparation of a uniform and stable dyed diesel oil mixture. Different volumes of dyed diesel oil were mixed with 50 mL of absolute ethanol and 100 mL of deionized water, resulting in diesel oil solutions of various concentrations. The absorbance of dyed diesel oil solution was measured by using an ultraviolet spectrophotometer (UV-2600), and the standard curve relating dyed diesel oil concentration and absorbance was drawn. The dyed diesel oil was added to the pulp for coal slurry adjustment tests. The absorbance of the supernatant of the samples was measured after downregulating the slurry under different test conditions, which allowed the calculation of the adsorption density of the collector on the particle surface. Equation (4) shows the formula for the adsorption density of the collector.

$$Q = \frac{V(C_0 - C_e)}{m} \tag{4}$$

where C_0 is the initial concentration of diesel oil; C_e is the residual concentration of diesel oil in the slurry; V is the volume of pulp, L; and m is the mass of the coal sample, g.

3. Results and discussion

3.1. Effect of single stage energy input on the flotation rate

Fig. 4 depicts the flotation results of high-ash tailings at varying stirring speeds. The yield of the flotation concentrate gradually increased as the stirring speed increased. The ash of the flotation concentrate increased with the stirring speed, and the lowest ash content was 21.37% at 1200 r/min. The yield of flotation tailings was generally approximately 50%, and the ash of flotation tailings was approximately 75%. The ash of the tailings increased by 52 % compared with that of the raw coal. The effect of stirring speed on the combustible recovery in 0–240 s is shown in Fig. 5. The combustible recovery at 1200 r/min was 75.93%, which was higher than that of 75.14% at 1500 r/min. Moreover, the lowest combustible

recovery was 70.59% at 600 r/min. Compared with the cumulative combustible recovery rate at other speeds, the 1200 r/min could achieve the highest combustible recovery.

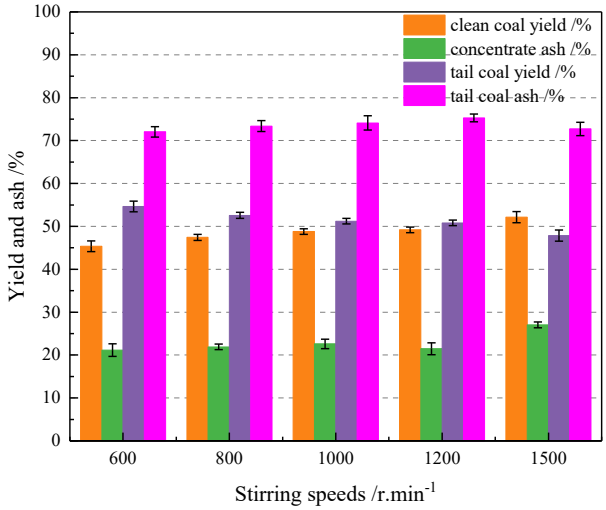

Fig. 4. Flotation results of high ash tail coal under different stirring speeds

The combustible recovery curve was fitted using the classical first-order kinetic model. Table 3 shows that the correlation coefficient R^2 of curve fitting was greater than 0.9924, suggesting that the data fitting results were highly accurate. The flotation rate constant increased gradually as the stirring speeds increased from 0.0183 s^{-1} to 0.0271 s^{-1}. It was slightly reduced to 0.0246 s^{-1} after 1200 r/min, indicating that the stirring speed significantly affected the flotation results. At 1200 r/min, the maximum flotation rate constant was 0.0271 s^{-1}, and the maximum combustible recovery was 74.35%.

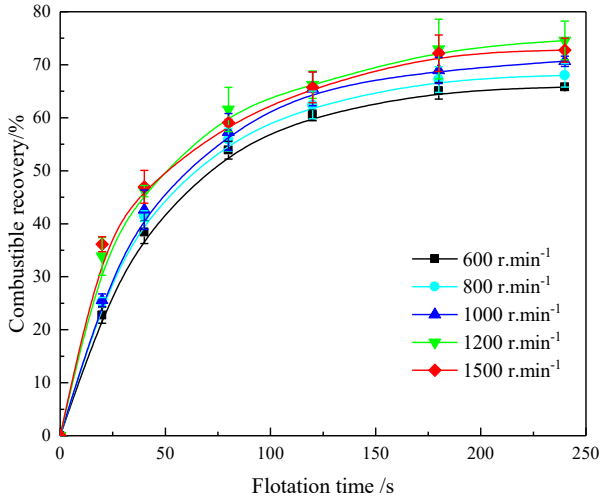

Fig. 5. Relationship between stirring speed and combustible recovery of flotation concentrate

3.2. Analysis of coal slime flotation effect in a short time

The flotation indicators at different stirring speeds for 40 s are shown in Table 4. Fig. 6 shows the relationship between clean coal yield and combustible recovery in 40 s. Table 4 and Fig. 6 show that, within a flotation time of 40 s, the yield and the combustible recovery of flotation concentrate increased gradually with the increase in stirring speed, and the combustible recovery at 600–1000 r/min had no noticeable change. Moreover, the combustible recovery of 50.19% was the highest at 1500 r/min.

In summary, the flotation rate constant and the maximum combustible recovery were the highest at 1200 r/min during the whole flotation time of 240 s. When the flotation time was within 40 s, the flotation concentrate yield and combustible recovery were the highest at 1500 r/min compared with other stirring speeds. The flotation process was continuous, in which the pulp concentration, phase composition, and interfacial chemical properties in the system changed nonlinearly. For the mechanical

flotation machine, the flotation process required uninterrupted energy input to complete the mixing and bubble mineralization processes. If the whole flotation process was carried out at the same speed, the flotation effect could not easily achieve the maximum recovery benefit. Therefore, reasonable energy input must be carried out according to the nonlinear variation characteristics of the flotation process to achieve the maximum benefit.

Table 3. Analysis of the effect of stirring speed on flotation kinetic parameters

n/r.min^{-1}	k/s^{-1}	R_∞/%	R^2
600	0.0183	68.4443	0.9931
800	0.0205	70.3740	0.9968
1000	0.0216	71.2436	0.9924
1200	0.0271	74.3489	0.9979
1500	0.0246	72.7388	0.9956

Table 4. Flotation indicators within 40 s of flotation time

n/r.min^{-1}	Y/%	Ac/%	R/%
600	25.46	17.05	41.67
800	26.83	17.81	43.51
1000	28.24	18.78	45.25
1200	30.04	18.54	48.28
1500	31.48	18.67	50.19

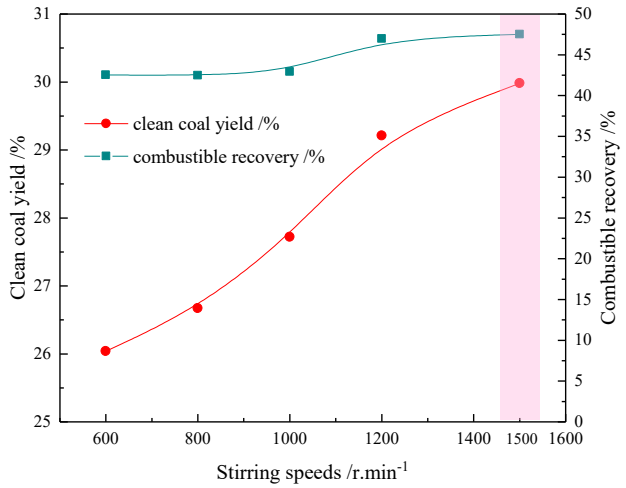

Fig. 6. Relationship between clean coal yield and combustible recovery within 40 s of flotation time

3.3. Effect of two-stage energy input on the flotation

The above experimental analysis showed that adjusting the speed of the flotation machine could effectively adapt the energy input to the coal slime's nonlinear physicochemical properties, resulting in the efficient recovery of fine coal slime from the slurry during the flotation process. Combined with the above test results, to facilitate the analysis of flotation results, we divided the separation process is divided into two stages. The first stage, referred to as the fast flotation period, ensured the flotation concentrate's quality. The second stage, the enhanced separation period, ensured the recovery of the flotation concentrate.

Four speeds of 1500, 1800, 2100, and 2400 r/min were selected under the two-stage energy input, and the total flotation time was 4 min., of which the fast flotation period was 40 s. The enhanced separation period was 200 s. Other test factors were consistent. Table 5 shows the speed configuration relationship between the fast flotation and enhanced separation periods. The speed of the improved separation period was higher than that of the fast flotation period.

Table 5. Adaptation of stirring speed during fast flotation and enhanced separation periods

Group	n/r.min^{-1}	
	Fast flotation periods (40 s)	Enhanced separation periods (200 s)
1	1500	1800
2	1500	2100
3	1500	2400
4	1800	2100
5	1800	2400
6	2100	2400

3.3.1. Experimental results

Fig. 7 illustrates the trend of combustible recovery with different stirring speeds in two stages. Combustible recovery also rose as the stirring speed increased during the fast flotation period. Conversely, during the enhanced separation period, a high stirring speed led to a low combustible recovery, showing the following order: $K_a<K_b<K_c$. The combustible recovery increased from 48.49% to 67.67% when the speed increased from 1500 to 2100 during the 40 s flotation period. Additionally, the stirring speed experienced a linear increase during the fast flotation period, yet the growth rate of combustible recovery decreased, specifically, $\Delta_1>\Delta_2$. Furthermore, $K_1>K_2>K_3$, $K_4>K_5>K_6$ indicated that the combustible recovery could be improved by enhancing the stirring speed in the enhanced separation period while maintaining the same stirring speed during the fast flotation period. The data fitting results under different energy inputs are shown in Table 6, indicating that the flotation time was divided into two stages. The goal of the overall combustible recovery was achieved by increasing energy input.

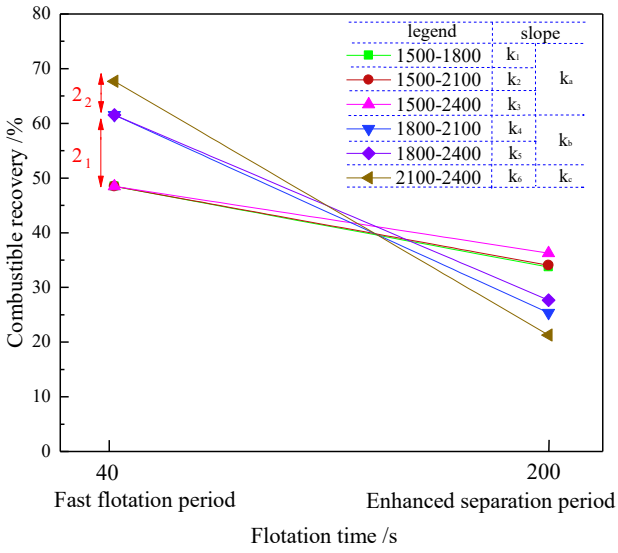

Fig. 7. Effect of two-stage stirring speed input on the combustible recovery of flotation concentration (Notes: The differences in combustible recovery between adjacent speeds were represented by Δ_1 and Δ_2 at a flotation time of 40 s. The absolute value of the slope of the corresponding speed curve was represented by K_1, K_2, K_3, K_4, K_5, and K_6. Among them, the slopes of the curves represented by K_1, K_2, and K_3 were generally represented by K_a. K_b represented the curves with slopes of K_4 and K_5. Kc represented the curves with slopes of K_6.)

The effects of stirring speed on the yield and combustible recovery of flotation concentrate are shown in Fig. 8. The yield of flotation concentrate rose with the increase in stirring speed, whereas the combustible recovery started to decline after increasing to 89.21%. Thus, a combustible recovery as high as 89.21% was achieved by setting the stirring speed at 1800 r/min in the fast flotation period and 2400 r/min in the enhanced separation period. The stirring speed had to be adjusted to match the nonlinear changes of pulp properties to ensure the highest overall combustible recovery.

Table 6. Data fitting results under different energy input

Equation	y = a + b · x					
Plot	1500-1800	1500-2100	1500-2400	1800-2100	1800-2400	2100-2400
Intercept	52.1800	52.1013	51.5428	70.5512	70.0035	79.2752
	k_1	k_2	k_3	k_4	k_5	k_6
Slope		k_a			k_b	k_c
	-0.0923	-0.0903	-0.0764	-0.2259	-0.2117	-0.2901

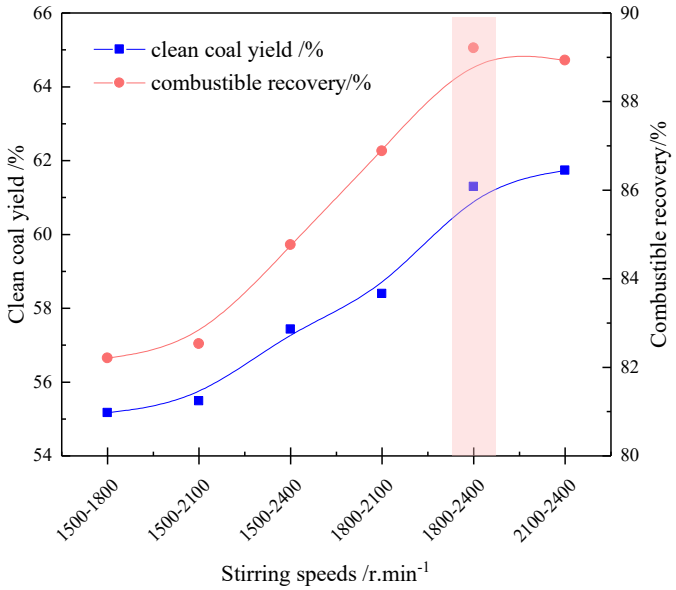

Fig. 8. Changes in the impact of stirring speed on flotation clean coal yield and combustible recovery under two levels of energy input

3.3.2. Granularity composition of flotation clean coal and tailings

Fig. 9 shows the cumulative weight distribution (a) and the fractional size distribution (b) of each particle size grade during the flotation period at varying stirring speeds. The results indicated that a high rotation speed of 2100 r/min was beneficial for the flotation of fine particles, whereas low stirring speeds of 1500 and 1800 r/min were favorable for the flotation of coarse particles. Specifically, the cumulative weights of less than 90% under the fast flotation period of 1500, 1800, and 2100 r/min were 197.3, 222.5, and 88.1 μm, respectively, as shown in Fig. 9(a). The content of fine particles was higher under a stirring speed input of 2100 r/min compared with the two cases of 1500 and 1800 r/min, as shown in Fig. 9(b). Our findings demonstrated that the content of particles greater than 100 μm in size in the flotation concentrate was between 5% and 6% under 1500 and 1800 r/min. Thus, a low stirring speed was conducive to the stability of coarse-grained bubble mineralized body, enhancing the flotation of coarse particles (Norori-McCormac, 2017). Conversely, a high stirring speed augmented the kinetic energy of fine particles, increasing the likelihood of collisions between fine coal slime and collector. Consequently, coarse particles floated to the surface preferentially, whereas fine particles underwent separation due to the intensifying effects of the high stirring speed (Koh and Smith, 2011).

Fig. 10 displays the distribution of the cumulative weight of clean coal (a) and the fractional size distribution (b) during the enhanced separation period under different stirring speeds. As shown in Fig. 10(a), during the enhanced separation period, the cumulative weights of less than 90% under the stirring speeds of 2100, 2400 (1800), and 2400 (2100) r/min were 55.3, 31.2, and 52.7 μm, respectively. Fig. 10(b) shows that the flotation products during the enhanced separation period at 2400 r/min (the fast flotation period of 1800) had a fine particle size. This finding suggested that the coarse clean coal particles already preferentially floated under a rotation speed of 1800 r/min during the fast flotation period. When

combining Figs. 9(a) and 10(a), the clean coal particles with a relatively coarse particle size preferentially floated out during the fast flotation period of fine coal separation. Meanwhile, the fine coal particles with a relatively fine particle size further separated under the high-speed shear action during the enhanced separation period. Overall, the particle size of clean coal flotation during the fast flotation period was larger than that during the enhanced separation period under any energy input.

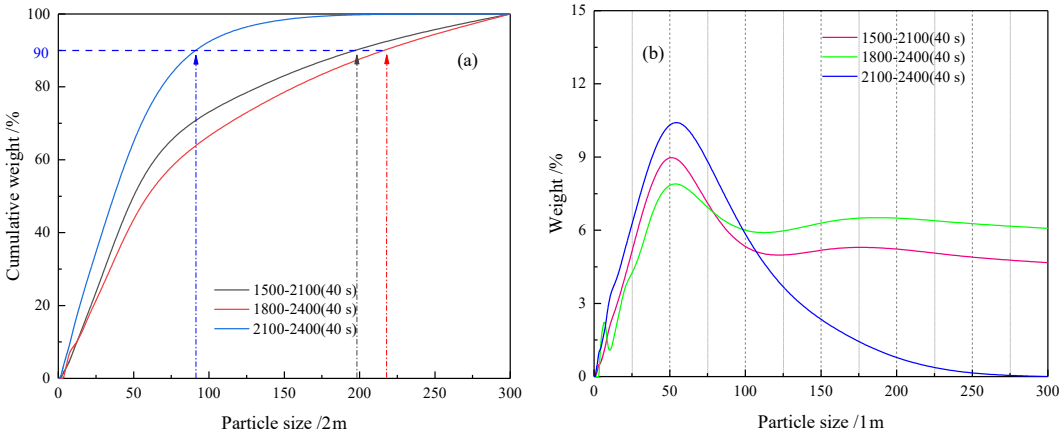

Fig. 9. Cumulative weight distribution (a) and fractional size distribution (b) of clean coal during the fast floatation period under different stirring speeds

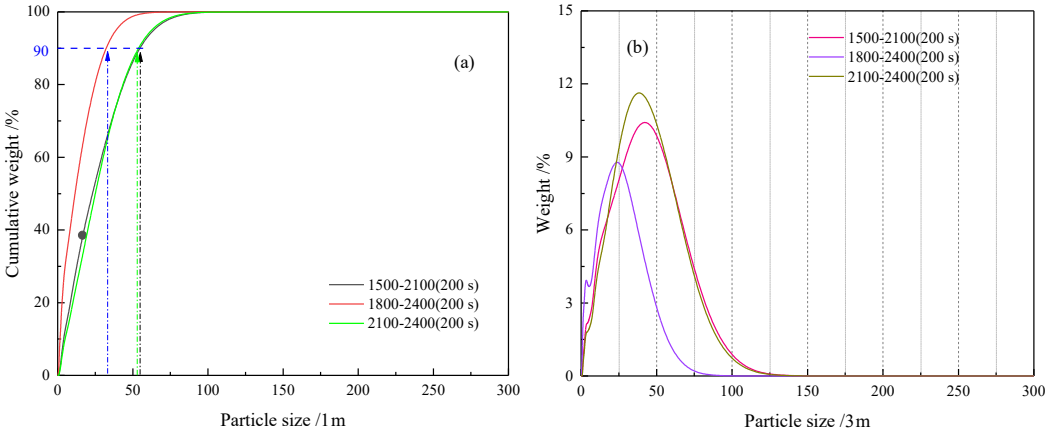

Fig. 10. Cumulative weight distribution (a) and fractional size distribution (b) of clean coal during the intensive separation period under different stirring speeds

Fig. 11(a) shows the cumulative weight of flotation tailings at different stirring speeds (a) and the corresponding percentage of each particle size class (b). Under the two-stage energy inputs of 1500–2100 r/min, the cumulative weight of flotation tailings with a particle size less than 90% was 21.7 μm. However, under the two-stage energy inputs of 1800–2400 and 2100–400 r/min, the cumulative weights of flotation tailings with a particle size less than 90% were 44.7 and 42.2 μm, respectively, indicating that the corresponding particle size distribution of flotation tailings in the two cases was close to each other. Fig. 11(b) shows that the particle size composition of tailings was relatively fine under the condition of 1500–22100 energy input. This finding was consistent with the results of the previous 1500–2100 r/min fast flotation and intensive separation periods, where coarse particles preferentially floated out, and fine particles were retained in the tailings, whereas the particle size distribution of tailings was close under the two conditions of 1800–2400 and 2100–2400 r/min. Therefore, the selection of 2100 r/min or 1800 r/min during the fast flotation period had a limited impact on the final particle size distribution of the flotation tailings. However, from the energy consumption perspective, combined with the flotation concentrate yield and recoveries of combustible matter under two-stage energy inputs in Fig. 8, performing flotation separation at 1800 r/min during the fast flotation period was more suitable than that at other conditions. The particle size of corresponding flotation tailings was relatively small under

1500–2100 r/min. Compared with the two other cases, 1500–2100 had a lower overall energy input, resulting in weaker turbulence intensity in the flow field. The weak turbulence state was less likely to destroy the already formed bubble mineralization structure, indicating that low energy input benefitted the structural stability of bubble mineralization and the flotation of coarse particles. Fine particles were more likely to remain in the tailings than coarse particles.

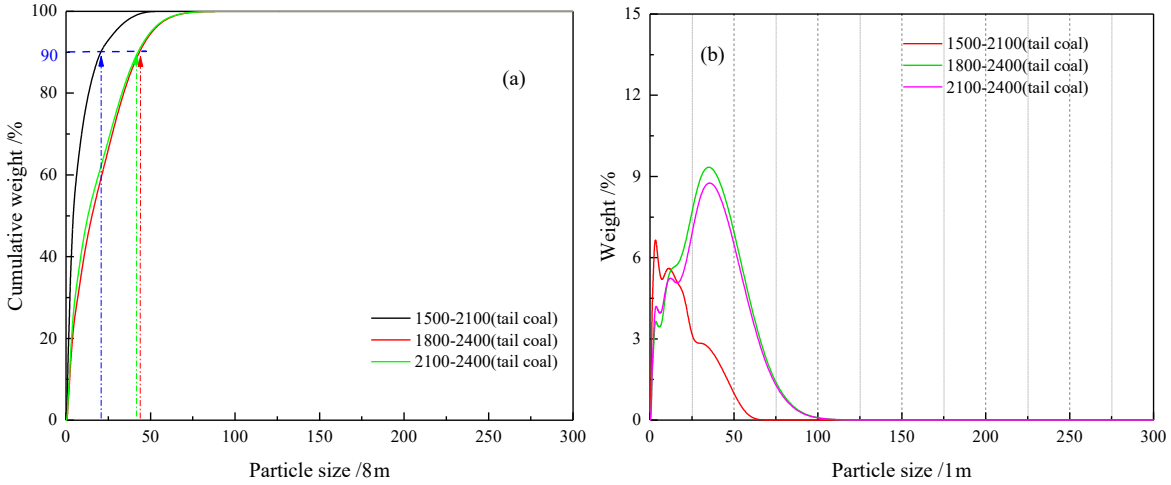

Fig. 11. Cumulative weight distribution (a) and fractional size distribution (b) of flotation tailings under different stirring speeds

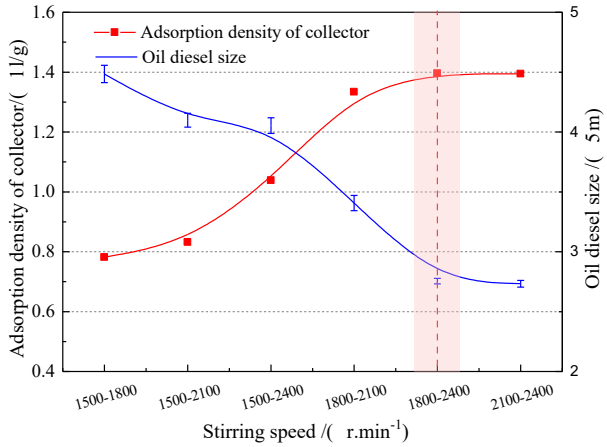

Fig. 12. Diesel oil droplet size distribution and its adsorption capacity on coal slime surface under two-stage energy input

3.3.3. Analysis of collector adsorption capacity and oil droplet size under two-stage energy input

The experimental results of diesel particle size distribution and its adsorption amount on coal slurry particles at two levels of energy input are shown in Fig. 12. The adsorption density of the diesel oil increased gradually with increasing stirring speed. The adsorption density of the diesel oil on coal particles reached a maximum of 1.40 μL/g for the two-stage energy at the stirring speed of 1800–2400 r/min, indicating that the stirring speed significantly affected the adsorption density of the oil droplets (Xue et al., 2023). However, the two-stage stirring speed combination of 2100–2400 r/min did not lead to any further increase in the adsorption density as compared with the1800–2400 r/min combination.

The effect of clay mineral stripping on the surface of oil droplets under different agitation intensities is shown in Fig. 14. Under high rotation speed, the clay minerals on the surface of the slime particles were fully scrubbed off, the hydrophobic adsorption sites on the surface of the coal particles were exposed, and the adsorption amount of the agent on the surface of the fine coal increased rapidly. Simultaneously, the turbulence intensity of the slurry improved, and the number of mutual collisions and effective collisions between particles increased, which facilitated oil droplets to break through the

hydration layer and clay mineral cover on the surface of coal particles (Wen et al., 2023). Moreover, as the distance between oil droplets and particles decreased, the potential energy increased, resulting in an energy barrier at a critical distance position. The oil droplets must overcome the energy barrier to adhere to the mineral surface, which increases the total potential energy among the oil droplets and particles, promoting the adsorption of oil droplets on the particle surface (Yang et al., 2020a). Thus, sufficient kinetic energy for oil droplets and particles, which requires external energy input, must be provided to improve the adsorption efficiency of oil droplets. Increasing the stirring speed is an important way to increase the adsorption kinetic energy of particles and oil droplets (Liu et al., 2023). However, with the continuous increase in the stirring speed, the particle size of the oil droplets continued to decrease, the flow around the oil droplets and particles became more pronounced, and the agent could not be adsorbed on the surface of the particles in time (Zhou et al., 2023). After analyzing the aforementioned reasons, this study concluded that energy input was beneficial in strengthening the dispersion of oil droplets, reducing the oil particle size, and promoting the adsorption of oil droplets on the surface of coal particles, thereby improving the efficacy of coal particle flotation. However, the energy input must be optimized to achieve optimal outcomes

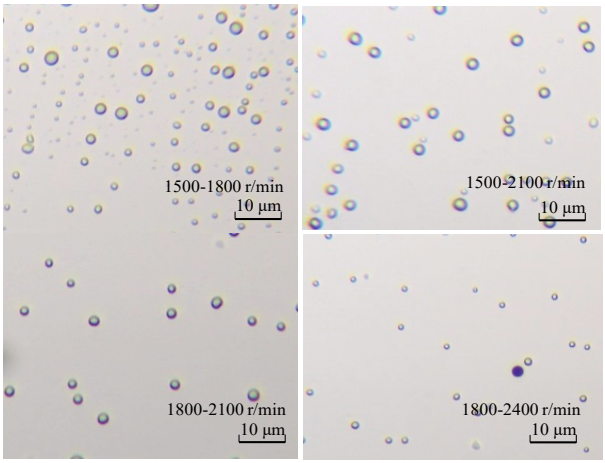

Fig. 13. Optical microscopic images of oil droplet size at different stirring speeds

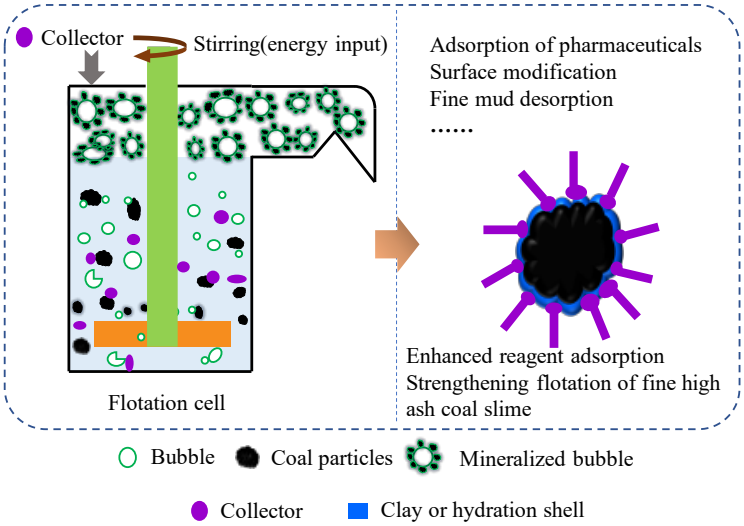

Fig. 14. Schematic of stirring intensity improving coal particle interface properties and enhancing chemical adsorption

4. Conclusions

(1) Flotation is a continuous process where the properties of pulp and the flow field environment undergo nonlinear changes. Solely relying on a constant energy input throughout the flotation

process may not optimize the recovery efficiency. Consequently, the energy input must be adjusted dynamically, in accordance with the nonlinear changes in pulp properties during the flotation process, to maximize the benefits of the flotation procedure.

(2) After 240 s of flotation, the maximum flotation rate constant of 0.0271 s^{-1} was reached at 1200 r/min, with the maximum combustible recovery of 74.35% under single-stage energy input, which was higher than that at 1500 r/min. However, when the flotation time was 40 s, the combustible recovery of 50.19% was the highest at 1500 r/min, higher than 46.97% at 1200 r/min.

(3) In the two-stage energy input mode, a low stirring speed favored the preferential flotation of coarse clean particles, and the fine clean coal particles were further separated during the enhanced separation stage. Consequently, the particle size of flotation concentrate in the rapid flotation period was larger than that in the enhanced separation period. The flotation process was conducted at 1800 r/min in the rapid flotation period and 2400 r/min in the enhanced separation period. At this time, the adsorption density of the collector on the surface of coal slime particles reached its maximum value of 1.40 μL/g, resulting in a combustible recovery of 89.21%.

Acknowledgements

The authors acknowledge the support of the National Nature Science Foundation of China (Grant no. 52074014), the Talent Introduction foundation of Anhui University of Science and Technology (Grant No. 13200419), the Open Foundation of State Key Laboratory of Mineral Processing (Grant No. BGRIMM-KJSKL-2024-08), the Provincial University Natural Science Foundation of Anhui (Grant No. KJ2020A0303) and the Foundation of Anhui Engineering Research Center for Coal Clean Processing and Carbon Emission Reduction.

References

ABBAKER, A. M. A., ASLAN, N., 2023, *The effect of microbubbles on coarse particle anionic flotation: analysis and optimization*. Physicochemical Problems of Mineral Processing, 59(6), 172298.

BARRAZA, J., GUERRERO, J., PIñERES, J., 2013, *Flotation of a refuse tailing fine coal slurry*. Fuel Process. Technol., 106, 498-500.

GUI, X., CAO, Y., XING, Y., YANG, Z., WANG, D., LI, C., 2017, *A two-stage process for fine coal flotation intensification*. Powder Technol., 313, 361-368.

GUO, H., HUANG, L., LIU, X., WANG, L., XIA, Y., CAO, Y., GUI, X., XING, Y., 2022, *Effect of different mass proportions of fine slime on the flotation performance of coal*. International Journal of Coal Preparation and Utilization, 43(11), 1863-1884.

HAN, Y., WANG, X., ZHU, J., WANG, P., 2022, *Gas Dispersion Characteristics in a Novel Jet-Stirring Coupling Flotation Device*. ACS Omega, 7(10), 9061-9070.

HASSANZADEH, A., SAFARI, M., HOANG, D. H., KHOSHDAST, H., ALBIJANIC, B., KOWALCZUK, P. B., 2022, *Technological assessments on recent developments in fine and coarse particle flotation systems*. Miner. Eng., 180, 107509.

HAZARE, G., PRADHAN, S. S., DASH, N., DWARI, R. K., 2023, *Studies on low-grade coking coal characterisation, flotation response and process optimisation*. International Journal of Coal Preparation and Utilization, 43(12), 2165-2187.

JUNG, M. U., KIM, Y. C., BOURNIVAL, G., ATA, S., 2023, *Industrial application of microbubble generation methods for recovering fine particles through froth flotation: A review of the state-of-the-art and perspectives*. Adv. Colloid Interface Sci., 322, 103047.

KADAGALA, M. R., NIKKAM, S., TRIPATHY, S. K., 2021, *A review on flotation of coal using mixed reagent systems*. Miner. Eng., 173, 107217.

KOH, P. T. L., SMITH, L. K., 2011, *The effect of stirring speed and induction time on flotation*. Miner. Eng., 24(5), 442-448.

LASKOWSKI, J. S., LIU, Q., O'CONNOR, C. T., 2007, *Current understanding of the mechanism of polysaccharide adsorption at the mineral/aqueous solution interface*. Int. J. Miner. Process., 84(1-4), 59-68.

LI, Z., CHANG, J., YANG, C., QU, J., YU, Y., XIONG, S., 2021, *Experiments and CFD simulation of accessories used in stirred pulp-mixing process*. Chemical Engineering and Processing - Process Intensification, 166, 108463.

LI, Z., ZHAO, C., ZHANG, H., LIU, J., YANG, C., XIONG, S., 2019, *Process intensification of stirred pulp-mixing in flotation*. Chemical Engineering and Processing-Process Intensification, 138, 55-64.

LIU, J., ZHANG, R., BAO, X., HAO, Y., GUI, X., XING, Y., 2023, *New insight into the role of the emulsified diesel droplet size in low rank coal flotation*. Fuel, 338, 127388.

NORORI-MCCORMAC, A., 2017, *The effect of particle size distribution on froth stability in flotation*. Sep. Purif. Technol., 184, 240-247.

OATS, W. J., OZDEMIR, O., NGUYEN, A. V., 2010, *Effect of mechanical and chemical clay removals by hydrocyclone and dispersants on coal flotation*. Miner. Eng., 23(5), 413-419.

PAN, G., ZHU, H., SHI, Q., ZHANG, Y., ZHU, J., OU, Z., GAO, L., 2023, *Effect of bubble trailing vortex on coal slime motion in flotation*. Fuel, 334, 126802.

SUN, L., CAO, Y., WANG, L., ZHENG, K., YAN, X., 2021, *Vortex-generator-induced intensification of fine mineral collection in pipe flow*. Miner. Eng., 171, 107116.

WAN, H., AN, Y., QU, J., ZHANG, c., XUE, J., WANG, S., BU, X. z., 2023, *Research on optimization method of flotation kinetic model based on molybdenite particle size effect*. Physicochemical Problems of Mineral Processing, 59(2), 163004.

WANG, H., LIANG, Y., LI, D., CHEN, R., YAN, X., ZHANG, H., 2022, *Collisional interaction process between a bubble and particles with different hydrophobicity*. Sep. Purif. Technol., 301, 121940.

WEN, P., MA, X., FAN, Y., DONG, X., CHEN, R., CHANG, M., BAI, X., CAI, S., 2023, *Insights into the interaction of polycarboxylate with coal and kaolinite and their application in flotation*. Fuel, 340, 127481.

XIA, Y., XING, Y., GUI, X., 2020a, *Oily collector pre-dispersion for enhanced surface adsorption during fine low-rank coal flotation*. Journal of Industrial and Engineering Chemistry, 82, 303-308.

XIA, Y., ZHANG, R., CAO, Y., XING, Y., GUI, X., 2020b, *Role of molecular simulation in understanding the mechanism of low-rank coal flotation: A review*. Fuel, 262, 116535.

XUE, Z., YANG, C., DONG, L., BAO, W., WANG, J., FAN, P., 2023, *Recent advances and conceptualizations in process intensification of coal gasification fine slag flotation*. Sep. Purif. Technol., 304, 122394.

YANG, L., LI, D., ZHANG, L., YAN, X., RAN, J., WANG, Y., ZHANG, H., 2020a, *On the utilization of waste fried oil as flotation collector to remove carbon from coal fly ash*. Waste Manag, 113, 62-69.

YANG, L., ZHU, Z., QI, X., YAN, X., ZHANG, H., 2018, *The Process of the Intensification of Coal Fly Ash Flotation Using a Stirred Tank*. Minerals, 8(12), 597.

YANG, Z., LIU, M., CHANG, G., XIA, Y., LI, M., XING, Y., GUI, X., 2020b, *Understanding the difficult selective separation characteristics of high-ash fine coal*. Physicochemical Problems of Mineral Processing, 56(5), 874-883.

YAO, N., LIU, J., SUN, X., LIU, Y., CHEN, S., WANG, G., 2021, *A Rational Interpretation of the Role of Turbulence in Particle-Bubble Interactions*. Minerals, 11(9), 1006.

YU, Y., MA, L., CAO, M., LIU, Q., 2017, *Slime coatings in froth flotation: A review*. Miner. Eng., 114, 26-36.

YUE, Z., REN, R., 2022, *Study on the influence mechanism of the grinding fineness on the floatability of coking middings*. Particulate Science and Technology, 41(1), 112-119.

ZHAO, G., FENG, B., QIU, T., ZHU, D., LI, X., GAO, Z., YAN, H., WU, H., 2022, *Enhanced flotation separation pyrrhotite from serpentine by fluid force field*. Colloids and Surfaces A: Physicochemical and Engineering Aspects, 651, 129711.

ZHOU, R., WANG, H., LI, X., LI, D., WANG, W., LIANG, Y., YAN, X., ZHANG, H., 2023, *Effect of energy input on flotation of particles with different sizes: Perspective of hydrodynamics characteristics*. Journal of Environmental Chemical Engineering, 11(6), 111272.

ZHUO, Q., LIU, W., WANG, P., DENG, J., XI, P., HUA, Y., 2023, *Influence of flotation reagents on separation mechanism of macerals: A multi-scale study*. Fuel, 333, 126480.